THE JOURNAL OF BIOLOGICAL CHEMISTRY VOL. 283, NO. 41, pp. 27636–27643, October 10, 2008

Disruption of the *Plasmodium falciparum PfPMT* Gene Results in a Complete Loss of Phosphatidylcholine Biosynthesis via the Serine-Decarboxylase-Phosphoethanolamine-Methyltransferase Pathway and Severe Growth and Survival Defects*

Received for publication, June 6, 2008, and in revised form, July 24, 2008 Published, JBC Papers in Press, August 11, 2008, DOI 10.1074/jbc.M804360200

William Harold Witola[‡], Kamal El Bissati[‡], Gabriella Pessi[‡], Changan Xie[§], Paul D. Roepe[§], and Choukri Ben Mamoun[‡1]

From the [‡]Department of Genetics and Developmental Biology, University of Connecticut Health Center, Farmington, Connecticut 06030 and the [§]Department of Chemistry and Department of Biochemistry, Cellular and Molecular Biology, Georgetown University, Washington, D. C. 20057

Biochemical studies in the human malaria parasite, *Plasmodium falciparum*, indicated that in addition to the pathway for synthesis of phosphatidylcholine from choline (CDP-choline pathway), the parasite synthesizes this major membrane phospholipid via an alternative pathway named the serine-decarboxylase-phosphoethanolamine-methyltransferase (SDPM) pathway using host serine and ethanolamine as precursors. However, the role the transmethylation of phosphatidylethanolamine plays in the biosynthesis of phosphatidylcholine and the importance of the SDPM pathway in the parasite's growth and survival remain unknown. Here, we provide genetic evidence that knock-out of the *PfPMT* gene encoding the phosphoethanolamine methyltransferase enzyme completely abrogates the biosynthesis of phosphatidylcholine via the SDPM pathway. Lipid analysis in knock-out parasites revealed that unlike in mammalian and yeast cells, methylation of phosphatidylethanolamine to phosphatidylcholine does not occur in *P. falciparum*, thus making the SDPM and CDP-choline pathways the only routes for phosphatidylcholine biosynthesis in this organism. Interestingly, loss of *PfPMT* resulted in significant defects in parasite growth, multiplication, and viability, suggesting that this gene plays an important role in the pathogenesis of intraerythrocytic *Plasmodium* parasites.

The protozoan parasite *Plasmodium falciparum* is the causative agent of the most severe form of human malaria, resulting in 300–500 million cases and 1–3 million deaths per year (1). The pathogenic stages of *P. falciparum* are those that invade mature erythrocytes, which are devoid of internal organelles and incapable of *de novo* lipid biosynthesis. Despite this, *P. falciparum* undergoes dramatic morphological and metabolic developmental changes and asexually divides to form up to 36 new daughter cells within 48 h of invading a human erythrocyte (2). This rapid multiplication of *P. falciparum* within host erythrocytes entails the active production of new plasma membranes in which phospholipids are major architectural and functional components. Phosphatidylcholine (PtdCho)[2] and phosphatidylethanolamine (PtdEtn), comprise 40–50% and 35–45%, respectively, of the parasite's total plasma membrane phospholipid content (3).

Genome data predict that *P. falciparum* possesses enzymatic pathways for the synthesis of all the necessary phospholipids from precursors transported from host milieu, such as serine, choline, inositol, glycerol, and fatty acids (3, 4). The synthesis of PtdCho in *P. falciparum* takes place via two metabolic pathways, the CDP-choline pathway (Kennedy pathway) and the serine-decarboxylase-phosphoethanolamine methyltransferase (SDPM) pathway (Fig. 1). In the SDPM pathway, ethanolamine (formed by the decarboxylation of serine by a parasite serine decarboxylase) is converted into phosphoethanolamine. The latter serves as a precursor for the synthesis of PtdEtn through the CDP-ethanolamine pathway and for the synthesis of PtdCho through the SDPM/CDP-choline pathways. Serine is readily available in the parasite cytosol due to the active degradation of host hemoglobin as well as uptake from the host milieu (5, 6).

The *PfPMT* gene in *P. falciparum* encodes the phosphoethanolamine methyltransferase that specifically methylates phosphoethanolamine to phosphocholine (p-Cho) via the SDPM pathway (7–9) (Fig. 1). p-Cho is then utilized by the CDP-choline pathway to synthesize PtdCho. The CDP-choline pathway also utilizes p-Cho synthesized from choline. PfPMT is a member of the PEAMT family of phosphoethanolamine methyltransferases that are also found in worms, plants, and other protozoa (7–9). The restricted phylogenetic distribution of this

* This work was supported, in whole or in part, by National Institutes of Health Grants AI51507 and AI51962. This research was also supported by Department of Defense Grant PR033005 as well as by Burroughs Wellcome Fund Award 1006267 (to C. B. M.). The costs of publication of this article were defrayed in part by the payment of page charges. This article must therefore be hereby marked "*advertisement*" in accordance with 18 U.S.C. Section 1734 solely to indicate this fact.

[1] Recipient of the Burroughs Wellcome Award, Investigators of Pathogenesis of Infectious Diseases. To whom correspondence should be addressed: Choukri Ben Mamoun, Dept. of Genetics and Developmental Biology, University of Connecticut Health Center, Farmington, CT 06030-3301. Tel.: 860-679-3544; Fax: 860-679-8345; E-mail: choukri@up.uchc.edu.

[2] The abbreviations used are: PtdCho, phosphatidylcholine; PtdEtn, phosphatidylethanolamine; SDPM, serine-decarboxylase-phosphoethanolamine-methyltransferase; p-Cho, phosphocholine; AdoMet, *S*-adenosyl-L-methionine; TdT, terminal deoxynucleotidyltransferase; TUNEL, TdT-mediated dUTP nick end labeling; SDCM, spinning disc confocal microscopy; RBC, red blood cell; PBS, phosphate-buffered saline; WT, wild type.

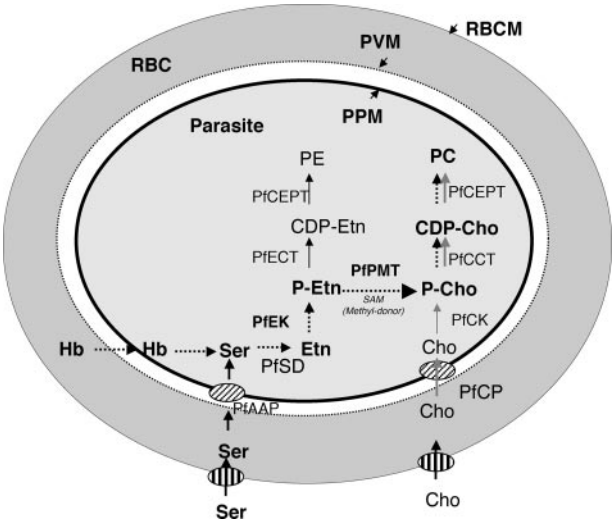

FIGURE 1. **Pathways for the biosynthesis of phosphatidylcholine in *P. falciparum*.** The CDP-choline pathway is shown with *gray arrows*. The SDPM pathway is depicted by *dotted arrows*. *PfAAP*, amino acid permease; *Cho*, choline; *CDP*, cytidine diphosphate; *CDP-cho*, CDP-choline; *CDP-Etn*, CDP-ethanolamine; *Hb*, hemoglobin; *PC*, phosphatidylcholine; *PE*, phosphatidylethanolamine; *PfCCT*, *P. falciparum* CTP phosphocholine cytidylyltransferase; *PfCEPT*, *P. falciparum* choline/ethanolamine-phosphate transferase; *PfCK*, *P. falciparum* choline kinase; *PfCP*, *P. falciparum* choline permease; *PfECT*, *P. falciparum* CTP phosphoethanolamine cytidylyltransferase; *PfEK*, *P. falciparum* ethanolamine kinase; *PfPMT*, *P. falciparum* phosphoethanolamine methyltransferase; *PPM*, parasite plasmamembrane; *PVM*, parasitophorous vacuolar membrane; *RBC*, red blood cell; *RBCM*, red blood cell membrane; *PfSD*, serine decarboxylase; *Ser*, serine; *SAM*, *S*-adenosyl-L-methionine.

class of enzymes suggests that they could be potential targets for the development of drugs to treat malaria and other parasitic diseases.

The physiological role PfPMT plays in parasite membrane lipid biogenesis and in the development and survival of intraerythrocytic *P. falciparum* is not fully understood. Here, we provide evidence that disruption of the *PfPMT* gene in *P. falciparum* completely abrogates the biosynthesis of PtdCho from serine and results in severe parasite growth and survival defects. Our findings show for the first time that the *in vivo* methylation of PtdEtn to PtdCho does not take place in *P. falciparum*, thus making the SDPM and CDP-choline pathways the main routes for PtdCho biosynthesis. Furthermore, the data define a novel role for PfPMT in the proliferation and survival of intraerythrocytic malaria parasites.

EXPERIMENTAL PROCEDURES

Plasmid Construction and Parasite Transfection—The plasmid *pRZ-TK-BSD2* (10) was used to construct the targeting vector *pW-pfpmt*Δ (Fig. 2). The *pRZ-TK-BSD2* plasmid encompasses the positive selectable marker *BSD* (blasticidin S deaminase) (11) from *Aspergillus terreus* that confers resistance to blasticidin and whose expression in *P. falciparum* is under the regulatory control of the *PcDT* (*Plasmodium chabaudi DHFR/TS*) promoter. The plasmid also harbors the negative marker *TK* (thymidine kinase) from herpes simplex that confers sensitivity to ganciclovir and whose expression is under the regulatory control of the *P. falciparum CAM* promoter. To construct the targeting vector *pW-pfpmt*Δ for *PfPMT* gene disruption, a 601-bp fragment (nucleotides 18–619 of the unspliced *PfPMT* gene sequence) (MAL13P1.214 PlasmoDB) was amplified by PCR and cloned at the HindIII/BlpI site upstream of the PcDT promoter in the *pRZ-TK-BSD2* plasmid. A second PCR was used to amplify a 505-bp fragment (nucleotides 650–1155 of the unspliced *PfPMT* gene sequence) for directional cloning at the EcoRI/NarI site downstream of the HrpII terminator in the *pRZ-TK-BSD2* plasmid. *P. falciparum* strain 3D7 was cultured in human red blood cells (RBCs) by the method of Trager and Jensen (12). Parasite transfection was done as previously described (13). After transfection, the cultures were maintained for an initial 48 h without blasticidin, and, thereafter, the drug was introduced in the cultures at 2.5 μg/ml final concentration. Cultures were continuously supplemented with 200 μM choline. The overall knock-out strategy (Fig. 2*A*) involved a two-step process by which the chromosomal *PfPMT* locus was first disrupted with the *BSD* cassette, after double cross-over homologous recombination, followed by elimination of the episome by selecting against expression of the *TK* gene with ganciclovir, a subversive substrate of the TK enzyme. To avoid loss of the knock-out parasites within the population (in the event that the SDPM pathway is an essential route for PtdCho biosynthesis), transfected parasites were continuously cultured in the presence of 200 μM choline, a concentration of choline ~20-fold greater than that present in human serum (14, 15). Transgenic parasites, selected on blasticidin and ganciclovir, were cloned by limiting dilution and genomic DNA from cloned parasites purified for molecular analysis using PCR and Southern and Western blotting to confirm the disruption of the *PfPMT* gene. *PfPMT* gene disruption at the chromosomal locus was analyzed using the primer pair PfPMT-F (5′-ATGACTTTG-ATTGAAAACTTAAACTCTG-3′) and PfPMT-R (5′-TTTGG-TGGCCTTAAAATAACCCCATCTTTGCA-3′).

A *PfPMT* add-back vector for *pfpmt*Δ complementation was generated by PCR amplification of the 801-bp full coding sequence of *PfPMT* from *P. falciparum* total cDNA. The fragment was directionally cloned at the XhoI site of a *pHC1* plasmid downstream of the *P. falciparum CAM* promoter. The *pHC1* vector harbors a *Toxoplasma gondii* dehydrofolate reductase gene that confers resistance to the selection drug, Pyrimethamine (16).

Southern Hybridization—Genomic DNA was extracted from wild type and transfected parasites, as previously described (11). About 2.5 μg of the genomic DNA was digested with HindIII, separated on a 1% agarose gel, and blotted onto a Nytran® SuperCharge nylon membrane (Whatman Schleicher and Schuell). Membranes were probed with [α-^{32}P]dCTP-labeled *PfPMT* and *BSD* gene probes.

Western Blot Analysis—Parasites were extracted from infected erythrocytes by treatment with 0.15% saponin and sonicated in PBS. The soluble fraction was separated on a 12% SDS-polyacrylamide gel and transferred to a nitrocellulose membrane. Immunoblotting was done using affinity-purified antibodies against PfPMT and the *P. falciparum* translation elongation factor-1α (PfEF-1α) as previously described (17).

Reverse Transcriptase-PCR—RNA was extracted from asynchronous parasites by TRIzol reagent (Invitrogen). Exactly 1 μg of total RNA was treated with DNase I (Invitrogen) to remove any contaminating DNA, followed by reverse transcription.

PfPMT was amplified from total cDNA using the primer pair PfPMT-F and PfPMT-R. As a loading control, the cDNA of the *PfTPXI* gene encoding the *P. falciparum* thioredoxin peroxidase (PF14_0368 in PlasmoDB 4.4) was amplified.

PfPMT Enzyme Activity Assay—Synchronous parasites were grown to 12% parasitemia and harvested at the trophozoite stage. Total extracts were prepared following sonication in extraction buffer (100 mM Hepes-KOH, pH 7.8, 5 mM dithiothreitol, 2 mM Na_2EDTA, 10% glycerol (v/v)) and centrifugation. The reaction mixture contained 100 mM Hepes-KOH, pH 8.6, 2 mM EDTA, 10% glycerol, 2 mM *S*-adenosyl-L-methionine (AdoMet), 1 mM phosphoethanolamine, 80 μM [*methyl*-^{14}C]AdoMet (400 nCi), and 50 μg of parasite protein extract in a total reaction volume of 100 μl. A blank reaction mixture lacked protein extract. The reaction mixtures were incubated for 30 min at 30 °C and terminated by the addition of 1 ml of ice-cold water. The products of the methylation reaction were purified through a AG (H^+) resin, following the method of Nuccio *et al.* (18) and quantified by liquid scintillation counting.

Labeling Assays and Phospholipid Analysis—Synchronized parasites cultured in medium without choline at 2% hematocrit were grown to 10% parasitemia at the early trophozite stage. The parasitized erythrocytes were resuspended in fresh medium containing either 1.6 μCi of [^{14}C]ethanolamine hydrochloride (51 mCi/mmol) or 0.1 μCi of [^{14}C]choline chloride (57 mCi/mmol) and cultured for 12 h. The infected erythrocytes were washed twice with PBS, and the pellet from a 60-ml culture volume was resuspended in a 20× volume of chloroform/methanol (2:1, v/v). Lipids were extracted by the Folch method (19), and the organic phase of the extract was evaporated and redissolved in 600 μl of chloroform/methanol (2:1). The organic extract (150 μl) was fractionated by two-dimensional TLC on Silica Gel-60 20 × 20-cm plates (Merck). For the first dimension, a solvent containing chloroform/methanol/ammonium hydroxide (84.5:45:6.5) was used. The second solvent was composed of chloroform/glacial acetic acid/methanol/water (90:30:6:2.6).

Parasite Growth Assays—Synchronized parasites at early ring stage were seeded at 2% parasitemia and cultured in the presence of 0, 10, 50, 100, 200, or 500 μM choline chloride for 96 h. Giemsa smears of the cultures were prepared at time points of 0, 12, 18, 32, 42, 56, and 96 h of culture, and the parasite counts and morphological state were determined by light microscopy.

Terminal Deoxynucleotidyltransferase (TdT)-mediated dUTP Nick End Labeling (TUNEL) Assay—The TUNEL kit (Roche Applied Science) was used to monitor cell survival following the manufacturer's instructions, with some modifications. Briefly, asynchronous cultures were grown to 10% parasitemia, and 1 ml of the culture aliquots was washed twice with PBS, and the cell number was adjusted to 1×10^6 cells/ml. Fixation was achieved by resuspending the cells in 2% paraformaldehyde solution in PBS and incubated at room temperature for 1 h. The fixed cells were washed twice with PBS, resuspended in 100 μl of 0.1% Triton X-100 in 0.1% sodium citrate solution, and incubated for 2 min on ice. Cells were then washed twice in PBS and kept on ice until labeling. A positive control sample was prepared by incubating fixed and permeabilized wild type (3D7) cells with 3000 units/ml of DNase I for 15 min at room temperature, followed by two washes with phosphate-buffered saline. To label the cells, 50 μl of the TUNEL reaction mixture was added to the cell pellet and mixed gently. A negative control sample was included by treating fixed, permeabilized wild type (3D7) cells with the labeling solution in the absence of the terminal TdT enzyme. The reaction mixtures were incubated in the dark at 37 °C for 1 h and then washed twice in PBS and resuspended in 250 μl of PBS. Cells were analyzed by fluorescence microscopy at 525 nm with the fluorescein isothiocyanate filter. To confirm that TUNEL staining correspond to cell death, parasites were grown in medium containing either 100 nM chloroquine or 100 nM pyrimethamine for 24 h and then processed for the TUNEL assay as described above.

Nuclei Counting by Spinning Disc Confocal Microscopy (SDCM)—Counting of nuclei by SDCM was done essentially as previously described for other strains of *P. falciparum* (20). In brief, all cultures were first synchronized three times by 5% D-sorbitol treatment, since multiple synchronization treatments successively improve the ring/early trophozoite ratio (20). Data were then routinely obtained 35–38 h after the last synchronization step, wherein segmented schizonts are clearly visible by light microscopy. We have previously described our customized SDCM apparatus in detail (20, 21). This instrument acquires "*z* stacks" for live cells at ~210–220 nm resolution (*x*, *y*, and *z*) in less than 1 s, which eliminates blurring due to parasite movement within the infected RBC. Along with reduced photobleaching and improved deconvolution procedures (20, 21), the method provides a reliable and convenient way to count nuclei for live intraerythrocytic schizonts using a Merzhauser motorized MS-2000 XY translation stage and an additional piezo table-optimized *z*-movement (5 mm/s over a range of 100 μm). Oil was DF-type (n = 1.515, low background fluorescence), and the camera was a Hamamatsu ORCA ER-cooled CCD with 1.3-megapixel full frame and 8.9 frames/s full rate. Excitation of SybrGreen-labeled nuclei (20) was with a Coherent Innova 300 I argon/krypton laser (300 milliwatts at 488 nm). Exposure was for 100 ms at 100 milliwatts laser power, and *z*-spacing was 200 nm (appropriate for iterative deconvolution as in Ref. 20. After iterative deconvolution using experimentally derived point spread functions, the *x*, *y* resolution of fluorescence SDCM data is only slightly lower than that of classical LSCM confocal data (measured on our instrument to be 213 nm using 520 nm light). *z* stack data were transferred to a Dell mini tower customized with three 750-Gb RAID array hard drives, and restoration was done using an Imaris 5.0.1/AutoQuant X software package from Bitplane Inc. (Saint Paul, MN), as described (20). *z*-Series of optical sections were deconvolved using the MLE method and a fixed point spread function routine with 15 iterations. Point spread function were obtained by mixing subresolution (d = 0.17 μm) fluorescent beads in cell culture. Restored images were transferred to Imaris and sorted into freely rotating three-dimensional objects in the "Surpass" mode, and nuclei counts were done with the aid of the "Spots" routine, which locates fluorescence peaks in three-dimensional space at operator-defined contrast half-width and intensity.

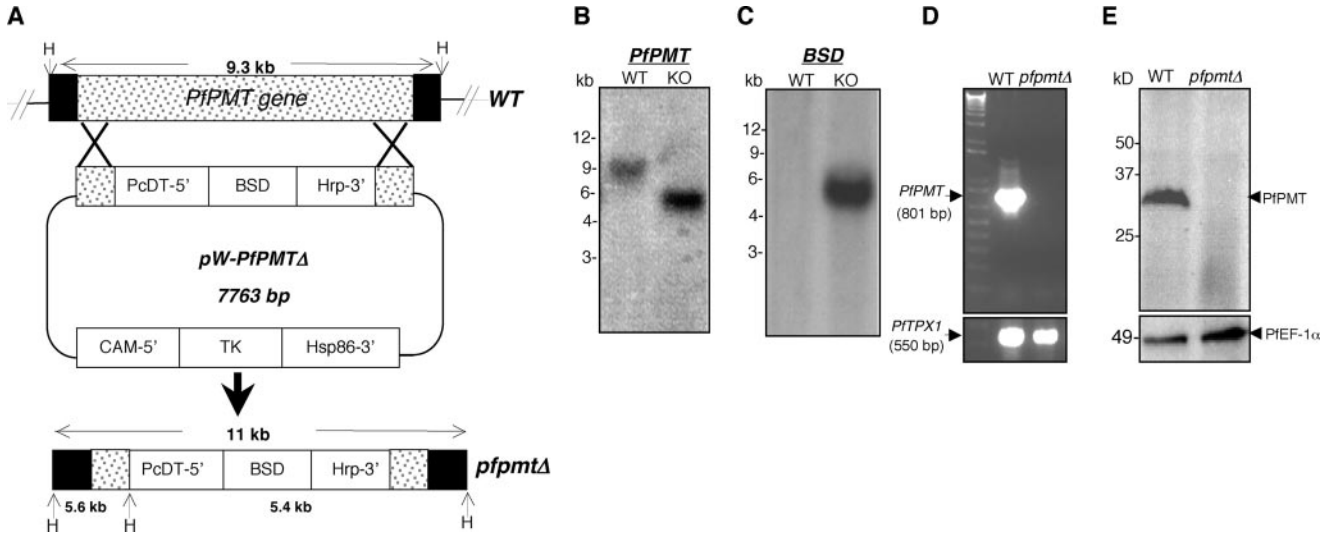

FIGURE 2. *A*, strategy for *PfPMT* gene disruption by double cross-over homologous recombination using a knock-out plasmid construct, *pW-pfpmt*Δ. The WT and the disrupted *PfPMT* gene (*pfpmt*Δ) loci are depicted with the HindIII (*H*) restriction sites used for Southern blot analysis. *PcDT-5′*, *P. chabaudi* dihydrofolate reductase/thymidylate synthase promoter; *BSD*, blasticidin S deaminase gene; *Hrp-3′*, histidine-rich protein gene terminator sequence; *Hsp86-3′*, heat shock protein 86 gene promoter; *CAM-5′*, *P. falciparum* calmodulin promoter; *TK*, thymidine kinase gene. *B–F*, characterization of the disruption of the *PfPMT* gene. *B*, Southern blot analysis of the HindIII-digested genomic DNA from the WT and knock-out (*pfpmt*Δ) parasites using the *PfPMT* gene probe. *C*, using the *BSD* gene probe, a 5.4-kb fragment excised by HindIII digestion is recognized only in the knock-out and not in the WT parasites. *D*, reverse transcription-PCR analysis of *PfPMT* transcription in WT and knock-out parasites. *E*, Western blot analysis of protein extracts from asynchronous cultures of WT and knock-out parasites using anti-Pfpmt and anti-PfEF-1α (loading control) antibodies.

Assignment of three-dimensional peaks as due to nuclei was confirmed by eye and then done in a semiautomated fashion to average across >200 schizonts in each case. Counts were exported to Excel or SigmaPlot software 9.0 for further statistical analysis.

RESULTS

Genetic Disruption of the PfPMT Gene in P. falciparum—To assess the physiological role of *PfPMT* in *P. falciparum*, we disrupted the *PfPMT* gene by homologous recombination. PCR analysis of genomic DNA from the cloned transgenic parasites demonstrated the replacement of the *PfPMT* gene by the *BSD*-containing targeting cassette in 10 individual clones. Southern blotting of HindIII-digested genomic DNA isolated from one clone (Fig. 2*B*) and using a 601-bp 5′-end *PfPMT* gene fragment probe (identical in sequence to that cloned in the *pW-pfpmt*Δ vector) showed the presence of 5.6- and 9.3-kb fragments in the *pfpmt*Δ and wild type parasites, respectively, confirming the disruption of the *PfPMT* gene locus in the *pfpmt*Δ parasites (Fig. 2, *B* and *C*). Additionally, probing with the *BSD* gene fragment revealed the expected 5.4-kb fragment in the *pfpmt*Δ parasites but not in the wild type (Fig. 2*C*), further confirming that gene replacement had occurred.

To test the loss of *PfPMT* expression in the selected *pfpmt*Δ clone, reverse transcription-PCR analysis was performed using primers within the *PfPMT* open reading frame. *PfPMT* cDNA could be detected using wild type but not *pfpmt*Δ RNA (Fig. 2*D*). As a control, the expression of the PfTPX1 gene was detected in both wild type and knock-out parasites. Analysis of the loss of *PfPMT* expression by immunoblotting using affinity-purified anti-PfPMT antibodies (17) showed that, although a 30 kDa PfPMT band was detectable in the wild type strain, there was no signal in the knock-out strain (Fig. 2*E*). As a loading control, antibodies raised against the parasite translation elongation factor, PfEF-1α (22), were used, and the expected ~49-kDa PfEF-1α band was found in both the wild type and *pfpmt*Δ strains (Fig. 2*E*).

*pfpmt*Δ *Parasites Lack PMT Activity and Cannot Synthesize PtdCho From Ethanolamine*—To determine whether *PfPMT* encodes the only phosphoethanolamine methyltransferase activity of *P. falciparum*, the three-step methylation of phosphoethanolamine to phosphocholine and the intermediate products was examined in protein extracts from either wild type or *pfpmt*Δ parasites using radiolabeled AdoMet as a methyl donor. As a control, we constructed a *pfpmt*Δ + *PfPMT* complemented strain, which expresses wild type *PfPMT* episomally in the *pfpmt*Δ strain. Whereas the formation of radiolabeled phosphocholine was readily detectable in reactions with extracts from the wild type and *pfpmt*Δ + *PfPMT* strains, phosphocholine could not be detected in the reaction mixture containing extracts from the *pfpmt*Δ parasites (Fig. 3*A*). Together, these results confirmed the loss of PfPMT enzymatic activity in the *pfpmt*Δ parasites and demonstrated that *PfPMT* encodes the only phosphoethanolamine methyltransferase activity in *P. falciparum*.

To determine how the loss of PfPMT affected SDPM-dependent synthesis of PtdCho, *in vivo* labeling assays with [^{14}C]ethanolamine in the wild type, *pfpmt*Δ, and complemented strains were performed in medium lacking choline. Two-dimensional TLC analysis of the parasite phospholipids following incubation with [^{14}C]ethanolamine revealed, as expected, the formation of radiolabeled PtdEtn in all three parasite strains (Fig. 3*B*, *top panels*). In contrast, the formation of radiolabeled PtdCho from [^{14}C]ethanolamine was only detectable in the wild type and *pfpmt*Δ + *PfPMT* parasites, not in the *pfpmt*Δ strain (Fig. 3*B*, *top panels*). Thus, disruption of PfPMT function results in a complete loss of the SDPM pathway. This result also demonstrates that *P. falciparum*, unlike mammalian

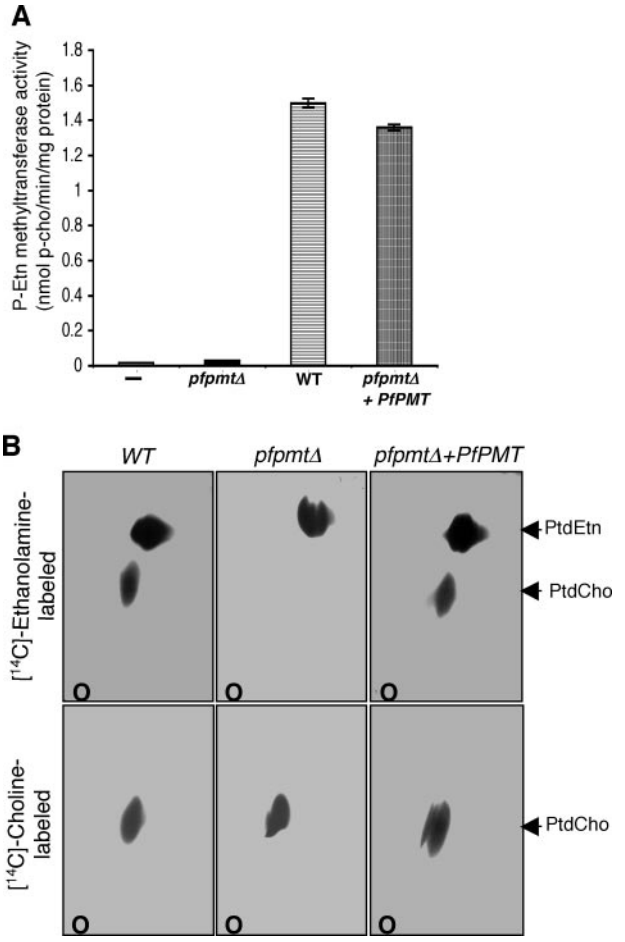

FIGURE 3. *A*, evidence for the loss of PfPMT enzymatic activity in the *pfpmt*Δ strain compared with the WT and *pfpmt*Δ + *PfPMT* strains. PfPMT activity in *P. falciparum* extracts (50 μg of total protein) was measured at 30 °C using phosphoethanolamine as substrate and AdoMet as co-substrate (methyl-donor). The product, phosphocholine, was purified using an AG-50(H^+) ion exchange resin. The formation of radiolabeled phosphocholine was quantified by scintillation counting, and the equivalent methyltransferase activity was derived. A reaction mixture without protein extract was included as a blank (−). Data are means ± S.D. derived from three independent experiments. *B*, synchronized WT, *pfpmt*Δ, and *pfpmt*Δ + PfPMT parasites grown to 10% parasitemia at early trophozoite stage in the absence of choline were labeled with either [^{14}C]ethanolamine (*top panels*) or [^{14}C]-choline (*bottom panels*) and incubated for 12 h. The infected erythrocytes were washed twice in PBS, and lipids were extracted by the Folch method (17). The organic phase of the lipid extracts were resolved by two-dimensional TLC, and signals were generated by autoradiography. ○, sample application point; *PtdEtn* and *PtdCho*, positions of phosphatidylethanolamine and phosphatidylcholine, respectively. *P-Etn*, phosphoethanolamine.

and yeast cells, cannot form PtdCho from PtdEtn. Labeling with [^{14}C]choline resulted in the incorporation of this substrate into PtdCho in all three strains (Fig. 3*B*, *bottom panels*), demonstrating that the CDP-choline pathway is not altered by the loss of PfPMT.

Loss of PfPMT Results in Growth and Morphological Defects That Are Only Partially Complemented by Choline—To examine the importance of PfPMT in the *P. falciparum* intraerythrocytic life cycle, the growth rate of *pfpmt*Δ parasites during their intraerythrocytic development and multiplication was compared with that of the wild type and *pfpmt*Δ + PfPMT strains. Since the SDPM and the CDP-choline pathways converge at the synthesis of phosphocholine from phosphoethanolamine and choline (Fig. 1), respectively, we envisaged that choline supplementation could complement any defects resulting from the loss of the *PfPMT* gene. The three strains were synchronized and cultured at 1% parasitemia in media containing increasing concentrations of choline for 48 h. Giemsa-stained parasite smears were analyzed by light microscopy (Fig. 4). Although similar parasite counts were found in the wild type and *pfpmt*Δ + *PfPMT* strains, the parasitemia in the *pfpmt*Δ culture was reduced by at least 50% at choline concentrations of 0, 10, and 50 μM in the culture medium (Fig. 4*A*). The addition of choline at 200 or 500 μM (10- and 25-fold higher than the physiological level, respectively) had only a marginal effect on growth of the *pfpmt*Δ (Fig. 4*A*) (data not shown). Wild type and *pfpmt*Δ + *PfPMT* parasites inoculated at 3% starting parasitemia and cultured for two consecutive generations in medium lacking choline increased their parasitemia to ~35%, whereas *pfpmt*Δ parasites reached only 10% parasitemia (Fig. 4*B*) under the same conditions (RBCs contain residual choline that can support limited parasite growth). These results indicated that choline supplementation at physiological levels could not rescue the loss of *PfPMT*, although a marginal rescue effect was notable at concentrations that were at least 10-fold the physiological level. Microscopic analysis of highly synchronized cultures indicated that, although the wild type and the *pfpmt*Δ + *PfPMT* strains progressed normally, the *pfpmt*Δ strain formed trophozoites and schizonts that were smaller in size and depicted a delayed progression rate (Fig. 4, *C* and *D*). Determination of the relative size of the mature schizonts by measuring the average RBC area occupied by the parasites showed that mature schizonts of the *pfpmt*Δ parasites occupied only about 33% of the RBC area, whereas their wild type and *pfpmt*Δ + *PfPMT* counterparts occupied ~75% of the RBC area (Fig. 4*E*).

*pfpmt*Δ *Parasites Have Altered DNA Replication*—The low number of daughter parasites produced during the intraerythrocytic life cycle of *pfpmt*Δ parasites could be due to a low number of nuclei produced during schizogony (and thus a low number of merozoites). Therefore, we quantified the number of nuclei from synchronized populations of live *pfpmt*Δ and *pfpmt*Δ + *PfPMT* parasites under continuous perfusion using DNA-targeted fluorophores and SDCM. The complemented strain (Fig. 5*A*) showed a Gaussian distribution of numbers of new nuclei per schizont that is similar to that measured previously for wild type parasites (20). In contrast, the *pfpmt*Δ strain grown in the absence of exogenous choline (Fig. 5*B*) showed a distinctly biphasic distribution of nuclei counts with the majority of schizonts showing a reduced number of nuclei consistent with microscopic analyses. Interestingly, when the *pfpmt*Δ strain was grown in the presence of exogenous choline (Fig. 5*C*), the distribution remained broadened but shifted to higher numbers of nuclei. These results suggest that efficient production of phosphocholine plays a role in the formation of new nuclei during schizogony. Similar results were obtained by flow cytometry (data not shown).

*pfpmt*Δ *Parasites Have Decreased Cell Viability*—To assess the effect of *PfPMT* disruption on the viability of intraerythrocytic parasites, asynchronous wild type, *pfpmt*Δ, and *pfpmt*Δ +

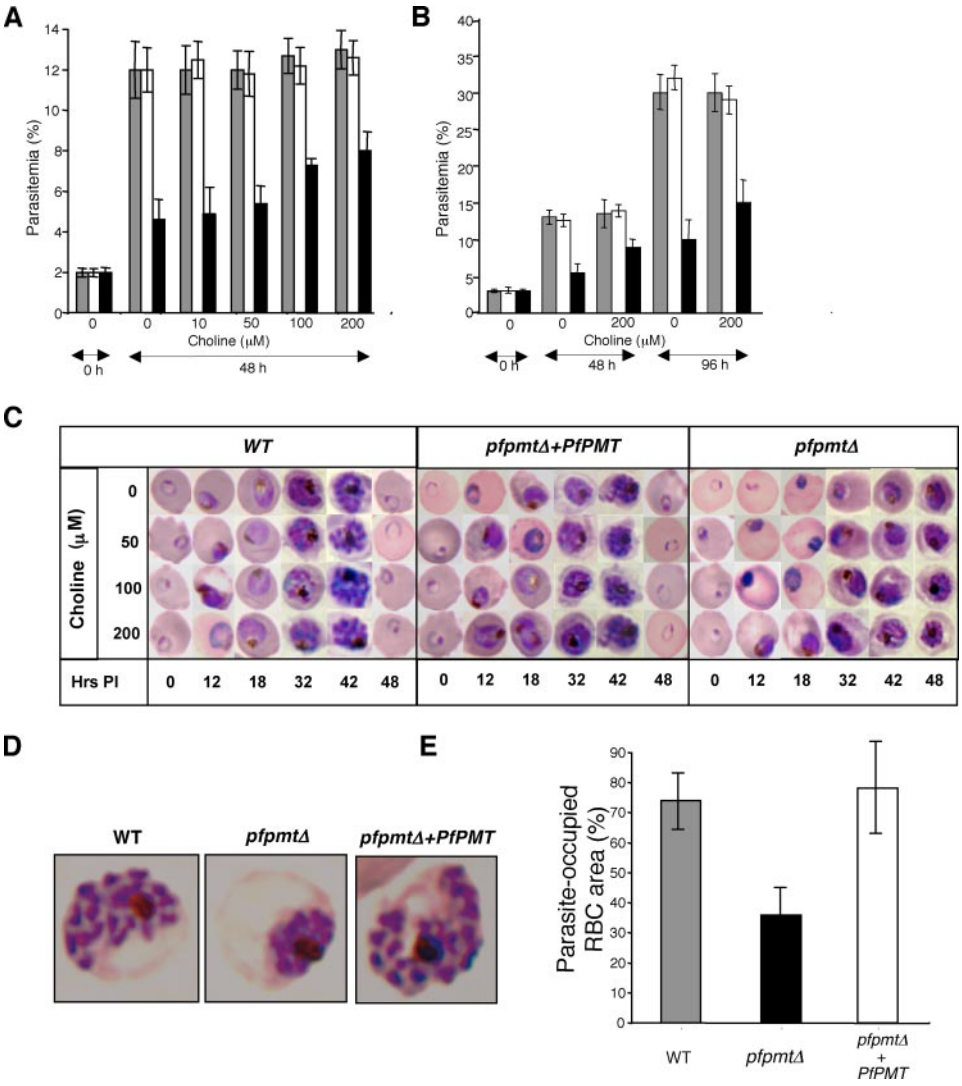

FIGURE 4. *A*, percentages of erythrocytes that were infected with WT, *pfpmt*Δ + PfPMT, and *pfpmt*Δ parasites (*gray*, *white*, and *black* columns, respectively) were determined by light microscopy on Giemsa-stained thin smears at 0 and 48 h of culture in medium with different concentrations of choline. One thousand RBCs were counted, and the percentage of parasitized cells was determined. (Based on *t* test analysis of the data, the difference between 0 and 200 μM choline was not significant.) Data are means ± S.D. of three independent experiments. *B*, parasitemia at 0, 48, and 96 h of culture in medium with 0 or 200 μM choline. *Gray*, *white*, and *black* columns represent parasitemia for the wild type, the *pfpmt*Δ + *PfPMT*, and *pfpmt*Δ parasite strains, respectively. Data are means ± S.D. of three independent experiments. (Based on *t* test analysis of the data, the difference between 0 and 200 μM choline was not significant.) *C*, progression of synchronized wild type, *pfpmt*Δ + *PfPMT*, and *pfpmt*Δ parasite strains grown at different concentrations of choline. The Giemsa-stained smears were prepared at different time points of culture (h postinvasion) as indicated and examined by light microscopy. One thousand RBCs were counted, and the percentage of parasitized cells was determined. The wild type and *pfpmt*Δ + *PfPMT* parasites that had reached the schizont stage at 42 h progressed to release new daughter parasites (merozoites) that then invaded previously uninfected RBCs to form the Ring stage of the parasites at 48 h. It should be noted that at this stage, there could have been some merozoites that were in the preinvasive stage and thus could not be easily detected microscopically. To be representative, at each time point and for each sample, 200 infected RBCs were examined, and the parasite morphology that was found to be consistent in at least 80% of the infected RBCs was taken as the representative morphology. *D*, representative images of schizonts for the wild type (*WT*), *pfpmt*Δ + *PfPMT*, and *pfpmt*Δ parasites. Five hundred parasites were analyzed for each form. *E*, comparison of the RBC area (percentage) occupied by a mature schizont stage of the WT, *pfpmt*Δ + *PfPMT*, and *pfpmt*Δ (*gray*, *white*, and *black columns*, respectively). The area was determined using ImageJ software (National Institutes of Health). Values are means of 10 different schizont-infected RBCs examined for each parasite strain, with S.D. values shown as *error bars*.

PfPMT parasites were analyzed by the TUNEL assay, which measures DNA fragmentation that occurs as an early event in cells undergoing cell death. Although a substantial number of *pfpmt*Δ parasites cultured in 0, 20, or 200 μM choline were positively stained with the TUNEL stain, wild type and *pfpmt*Δ + *PfPMT* parasites cultured under similar conditions were not (Fig. 6*A*). As a control, wild type parasites treated with DNase I to induce chromosomal DNA strand breaks stained positively in the presence of the TdT enzyme but negatively when the TdT enzyme was omitted from the reaction (Fig. 6*B*). To ensure that TUNEL staining correlates with parasite death, wild type, *pfpmt*Δ, and *pfpmt*Δ + *PfPMT* parasites were treated with 100 nM chloroquine or 100 nM pyrimethamine (concentrations ~10-fold above their IC_{50} values) for 24 h and subjected to the TUNEL assay. In all cases, the drug-treated parasites showed a positive TUNEL staining (Fig. 6*C*). Taken together, these results suggest that PfPMT plays an important role in the parasite's viability.

DISCUSSION

The results presented here show that *P. falciparum* parasites lacking PfPMT are unable to synthesize their major phospholipid, PtdCho, via the SDPM pathway, and display major alterations in parasite development, multiplication, and survival. Furthermore, this study provided the first genetic evidence that, unlike mammalian and yeast cells, *P. falciparum* parasites lack the ability to form PtdCho from PtdEtn.

PfPMT is a member of a new class of AdoMet-dependent methyltransferases found in *Caenorhabditis elegans* and plants. No homologs exist in mammals (23–27). Although they share significant homology in their primary structure, these enzymes differ in the structural organization of their catalytic domains. The plant PEAMTs have two tandem catalytic domains, with the N-terminal domain catalyzing methylation of phosphoethanolamine into monomethylphosphoethanolamine and the C-terminal domain acting in the last two methylation reactions to form phosphocholine (23, 24). *C. elegans* PEAMTs contain only one methyltransferase domain located in either the N-terminal end of the protein, in the

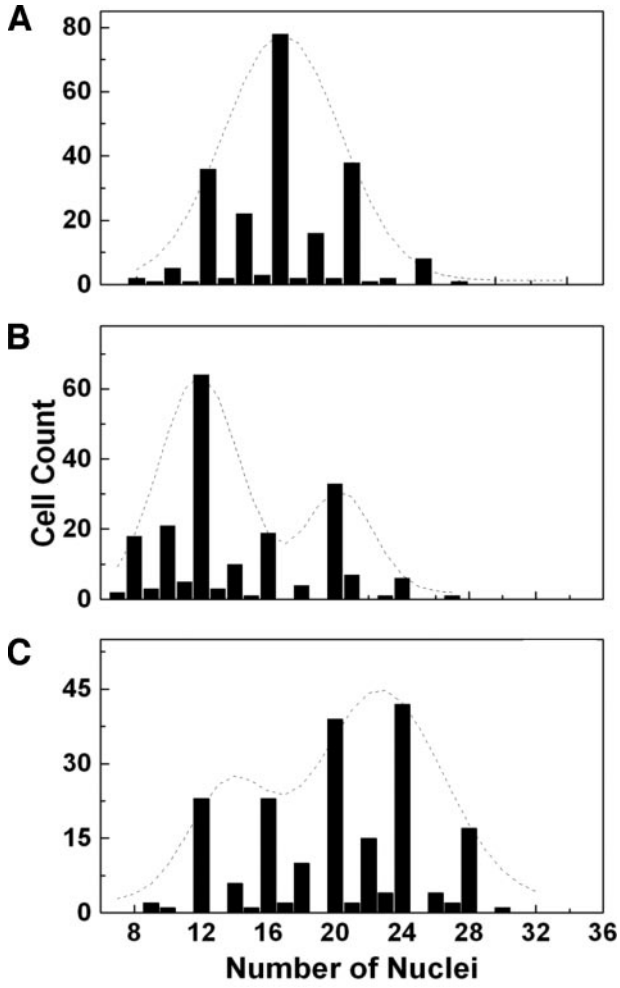

FIGURE 5. **Determination of nuclei counts for live parasitized RBCs by spinning disc confocal microscopy.** *A*, population of 220 RBCs infected with *pfpmt*Δ + PfPMT parasites in medium without choline. *B*, population of 198 RBCs infected with *pfpmt*Δ parasites cultured in medium without choline. *C*, population of 194 RBCs infected with *pfpmt*Δ parasites cultured in medium containing 21 μM choline.

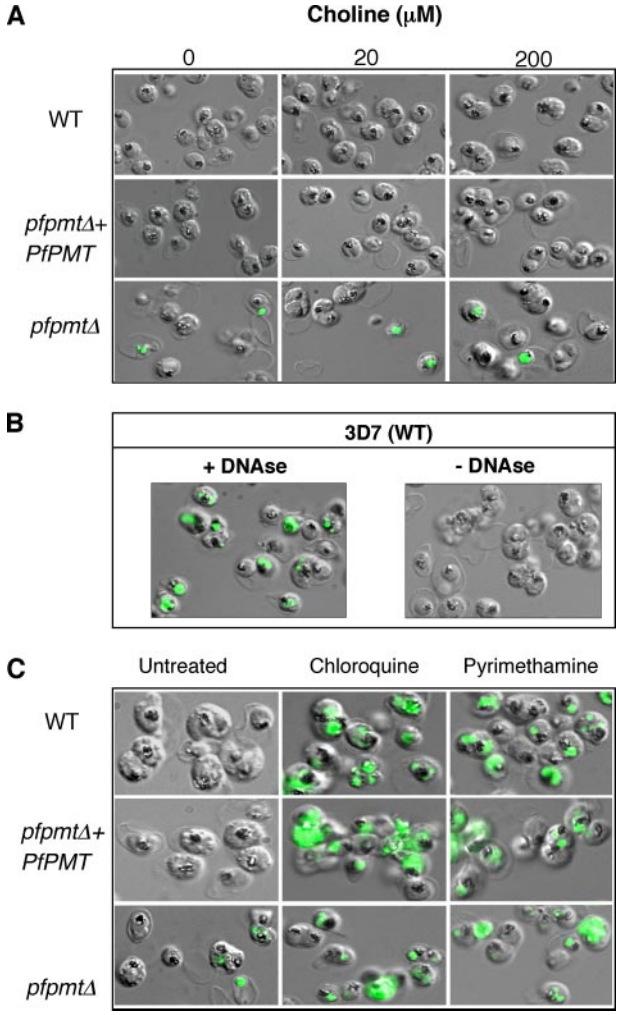

FIGURE 6. **TUNEL assay to monitor DNA fragmentation and parasite viability.** *A*, WT, *pfpmt*Δ + *PfPMT* and *pfpmt*Δ parasites cultured in medium with different concentrations (0, 20, and 200 μM) of choline and tested by TUNEL staining. The seemingly higher than 10% parasitemia is due to permeabilization conditions that reduce the number of uninfected red blood cells. *B*, positive (DNase-treated) and negative (no DNase) controls for TUNEL staining in WT parasites. *C*, WT, *pfpmt*Δ + *PfPMT*, and *pfpmt*Δ parasites were cultured in the presence of either 100 nM pyrimethamine or 100 nM chloroquine for 24 h and tested for apoptosis by the TUNEL assay.

case of Pmt1, or in the C-terminal end of the protein in Pmt2 (25, 26). Pmt1 catalyzes only the first methylation reaction, whereas Pmt2 catalyzes the last two methylation reactions. The *Plasmodium* PfPMT shares homology with both plant and *C. elegans* PEAMTs (Pmt1 and Pmt2) but is only half the size of these proteins and catalyzes all three methylation steps (7). The properties of these enzymes and their absence in mammals suggests that, if validated, they would be viable targets for developing antiprotozoan and antihelmintic therapies (7, 25). Metabolic studies using radiolabeled ethanolamine showed that although wild type, knock-out, and complemented parasite strains synthesized PtdEtn from ethanolamine, only wild type and complemented parasites formed PtdCho from this precursor. Interestingly, radiolabeled choline was incorporated to similar levels into PtdCho in the three strains, suggesting that neither the CDP-choline pathway nor the transport of choline is affected in the *pfpmt*Δ knock-out parasite. Together, the metabolic studies demonstrate that the transmethylation of PtdEtn to form PtdCho does not occur in *P. falciparum* and that the SDPM pathway is the sole pathway used by the parasite to synthesize PtdCho from ethanolamine. This is further supported by the fact that no intermediates of the transmethylation of PtdEtn (monomethyl-PtdEtn and dimethyl-PtdEtn) can be identified in wild type parasites labeled with ethanolamine and that PfPMT *in vitro* or expressed in yeast cells lacks the ability to catalyze the transmethylation of PtdEtn (7, 8). Together the data suggest that the SDPM pathway might be a significant source of phosphocholine used for the biosynthesis of PtdCho in *P. falciparum*, as is the case in plants (28). This is consistent with the previous observation that *P. falciparum* develops and propagates normally in culture medium without choline (29, 30). Interestingly, *C. elegans* with a knocked down phosphoethanolamine *N*-methyltransferase had severe developmental defects and a drastic reduction in fertility that could not be rescued by the addition of superphysiological levels of choline (26), suggesting that the

physiological importance of PEAMTs is conserved across kingdoms.

Whereas the lipid labeling studies confirmed the essential function of the SDPM pathway in the synthesis of PtdCho in the absence of choline, the loss of *PfPMT* was not lethal when choline was not added to the culture medium. The survival of knock-out parasites under these conditions is most likely due to the presence of residual choline in human erythrocytes. Nevertheless, loss of PfPMT resulted in significant reduction (~50%) in parasite progeny that was only marginally rescued by choline supplementation even when choline was added at 25 times the physiological concentration (7–20 μM) (12, 13).

Analysis of parasite progression into schizogony indicated that *pfpmt*Δ parasites had a delayed rate of nuclear division and formed fewer nuclei per infected erythrocyte than the wild type and complemented parasites (Fig. 5). Furthermore, of the parasites that progressed through the intraerythrocytic life cycle, a substantial percentage underwent DNA degradation, as revealed by TUNEL staining (Fig. 6). Treatment of wild type parasites, which are uniformly TUNEL-negative, with lethal doses of chloroquine or pyrimethamine (all three strains are sensitive to these compounds) resulted in positive TUNEL staining, indicating that this assay detected dying and/or dead parasites. Together, these findings indicate that disruption of *PfPMT* results in defective parasite growth and multiplication as well as reduced parasite viability.

In *S. cerevisiae*, the loss of the *PEM1* and *PEM2* genes encoding phospholipid methyltransferases responsible for the synthesis of PtdCho from PtdEtn results in choline auxotrophy. Choline supplementation restores the growth of the mutant to wild type levels (31, 32). In contrast, whereas choline incorporation into PtdCho was similar in the wild type, knock-out and complemented parasites, choline supplementation only partially complemented the growth, multiplication, and survival defects of *pfpmt*Δ parasites. Two possible hypotheses could account for these major differences. First, PfPMT might contribute to the synthesis of a pool of PtdCho that is structurally different from that synthesized via the CDP-choline pathway and that might play a critical role in membrane biogenesis and/or signaling during the parasite's intraerythrocytic growth and proliferation.

Alternatively, the intermediates of the transmethylation of phosphoethanolamine (monomethyl-phosphoethanolamine and dimethyl-phosphoethanolamine) could function as signaling molecules during the parasite's life cycle, controlling various cellular processes, such as parasite size, DNA replication, multiplication, and survival. Future cell biological and genomic studies will aim to distinguish between these hypotheses and unravel the mechanism by which PfPMT controls growth, proliferation, and survival of *P. falciparum*.

Altogether, the studies presented here show that PfPMT is important for membrane biogenesis, development, survival, and propagation of the parasite. Compounds that target PfPMT could thus be combined with those that specifically target choline transport, choline phosphorylation, or other steps of the CDP-choline pathway in order to completely block PtdCho biosynthesis and kill the parasite.

Acknowledgments—We are grateful to Harriet Zawistowski (General Clinical Research Center, University of Connecticut Health Center) for technical assistance. We thank Dr. Sachiko Takebe for the purification of the PfPMT antibodies, Gene Pizzo for help with fluorescence-activated cell sorting analysis, and Dr. Megan Downie for comments on the manuscript.

REFERENCES

1. World Health Organization (2000) *WHO Tech. Rep. Ser.* **892,** 1–74
2. Krishna, S. (1997) *Br. Med. J.* **315,** 730–732
3. Vial, H. J., and Ben Mamoun, C. (2005) in *Molecular Approaches to Malaria* (Sherman, I. W., ed) pp. 327–352, American Society for Microbiology Press, Washington, D. C.
4. Holz, G. G. (1977) *Bull. W. H. O.* **55,** 237–248
5. Francis, S. E., Banerjee, R., and Goldberg, D. E. (1997) *J. Biol. Chem.* **272,** 14961–14968
6. Kirk, K. (2001) *Physiol. Rev.* **81,** 495–537
7. Pessi, G., Kociubinski, G., and Mamoun, C. B. (2004) *Proc. Natl. Acad. Sci. U. S. A.* **101,** 6206–6211
8. Pessi, G., Choi, J. Y., Reynolds, J. M., Voelker, D. R., and Mamoun, C. B. (2005) *J. Biol. Chem.* **280,** 12461–12466
9. Pessi, G., and Ben Mamoun, C. (2006) *Future Lipidol.* **1,** 173–180
10. El Bissati, K., Zufferey, R., Witola, W. H., Carter, N. S., Ullman, B., and Ben Mamoun, C. (2006) *Proc. Natl. Acad. Sci. U. S. A.* **103,** 9286–9291
11. Mamoun, C. B., Gluzman, I. Y., Goyard, S., Beverley, S. M., and Goldberg, D. E. (1999) *Proc. Natl. Acad. Sci. U. S. A.* **96,** 8716–8720
12. Trager, W., and Jensen, J. B. (1976) *Science* **193,** 673–675
13. Fidock, D. A., Nomura, T., and Wellems, T. E. (1998) *Mol. Pharmacol.* **54,** 1140–1147
14. Zeisel, S. H., Growdon, J. H., Wurtman, R. J., Magil, S. G., and Logue, M. (1980) *Neurology* **30,** 1226–1229
15. Zeisel, S. H. (2000) *J. Am. Coll. Nutr.* **19,** 528S–531S
16. Crabb, B. S., Triglia, T., Waterkeyn, J. G., and Cowman, A. F. (1997) *Mol. Biochem. Parasitol.* **90,** 131–144
17. Witola, W. H., Pessi, G., El Bissati, K., Reynolds, J. M., and Mamoun, C. B. (2006) *J. Biol. Chem.* **281,** 21305–21311
18. Nuccio, M. L., Ziemak, M. J., Henry, S. A., Weretilnyk, E. A., and Hanson, A. D. (2000) *J. Biol. Chem.* **275,** 14095–14101
19. Folch, J., Lees, M., and Sloane Stanley, G. H. (1957) *J. Biol. Chem.* **226,** 497–509
20. Gligorijevic, B., Purdy, K., Elliott, D. A., Cooper, R. A., and Roepe, P. D. (2008) *Mol. Biochem. Parasitol.* **159,** 7–23
21. Gligorijevic, B., McAllister, R., Urbach, J. S., and Roepe, P. D. (2006) *Biochemistry* **45,** 12400–12410
22. Mamoun, C. B., and Goldberg, D. E. (2001) *Mol. Microbiol.* **39,** 973–981
23. Bolognese, C. P., and McGraw, P. (2000) *Plant Physiol.* **124,** 1800–1813
24. Charron, J. B., Breton, G., Danyluk, J., Muzac, I., Ibrahim, R. K., and Sarhan, F. (2002) *Plant Physiol.* **129,** 363–373
25. Palavalli, L. H., Brendza, K. M., Haakenson, W., Cahoon, R. E., McLaird, M., Hicks, L. M., McCarter, J. P., Williams, D. J., Hresko, M. C., and Jez, J. M. (2006) *Biochemistry* **45,** 6056–6065
26. Brendza, K. M., Haakenson, W., Cahoon, R. E., Hicks, L. M., Palavalli, L. H., Chiapelli, B. J., McLaird, M., McCarter, J. P., Williams, D. J., Hresko, M. C., and Jez, J. M. (2007) *Biochem. J.* **404,** 439–448
27. Brendza, K. M., Haakenson, W., Cahoon, R. E., Hicks, L. M., Palavalli, L. H., Chiapelli, B. J., McLaird, M., McCarter, J. P., Williams, D. J., Hresko, M. C., and Jez, J. M. (2007) *Biochem. J.*
28. Mudd, S. H., and Datko, A. H. (1986) *Plant Physiol.* **82,** 126–135
29. Mitamura, T., Hanada, K., Ko-Mitamura, E. P., Nishijima, M., and Horii, T. (2000) *Parasitol. Int.* **49,** 219–229
30. Witola, W. H., and Ben Mamoun, C. (2007) *Eukaryot. Cell* **6,** 1618–1624
31. Kodaki, T., and Yamashita, S. (1987) *J. Biol. Chem.* **262,** 15428–15435
32. Summers, E. F., Letts, V. A., McGraw, P., and Henry, S. A. (1988) *Genetics* **120,** 909–922